SSRG International Journal of Electrical and Electronics Engineering
ISSN: 2348-8379/ https://doi.org/10.14445/23488379/IJEEE-V12I4P114

Volume 12 Issue 4, 201-209, April 2025

Original Article

Frequency Stability and Performance Analysis of Grid Forming Inverter in Grid-Tied Mode Using AC Current Limitation

Hetal Desai[1], Shweta Dour[2], Pramod Modi[3]

[1,2]*Electrical and Electronics Engineering Department, Navrachana University, Gujarat, India.*
[3]*Electrical Engineering Department, M.S.University of Baroda, Gujarat, India.*

[1]*Corresponding Author : hetal.desai1704@gmail.com*

Received: 10 February 2025 Revised: 12 March 2025 Accepted: 14 April 2025 Published: 29 April 2025

Abstract - *Integrating renewable distributed generation with a grid-tied Grid Forming Inverter (GFI) in AC power systems is essential for voltage amplitude and frequency stability. Frequency stability and its performance are governed by classical mechanics in AC power systems having high inertia. Grid-Forming Inverter control strategy is widely accepted by researchers for seamless integration with renewable distributed generation networks. The prime advantage of the GFI control strategy is low inertia compared to conventional Synchronous Machines (SMs). As a result, it provides a fast control response to maintain system stability incorporated due to Synchronous Machines (SMs). An inverter may be compelled to operate in a current-limiting mode that modifies inverter dynamics during grid emergencies like faults, voltage decreases, or frequency and phase jumps. As a result, it is susceptible to losing grid synchronization. In this paper, the system of Synchronous Machine and GFI (low inertia) with AC current limitation control strategy is being introduced. To maintain an appropriate power profile, mitigate load disturbances and limit over current, the AC current limit technique in GFI is used, which introduces reference current restricted to the maximum (Saturated) allowable current value. Frequency stability is taken as a performance parameter here. MATLAB Simulink simulates complete systems with SMs, Droop Control Strategy at SMs side, GFI with voltage and current loop to generate switching time, and AC current limitation techniques. The frequency, voltage and power dynamics have been studied for load disturbance conditions.*

Keywords - *Droop control, Grid forming inverter, AC current limiter, inertia, Frequency stability.*

1. Introduction

The most important concern in the modern world is sustainability. Global power grid suppliers are developing various ways to create a sustainable and green environment. The most challenging part of integrating more inverter-based sources, such as solar, wind, and battery storage systems, with a grid that uses them is grid synchronization. Because it is very low or nonexistent, it will lead to significant voltage and frequency fluctuations and erratic grid operation. This could result in load or trip IBRs. There may also be problems with the electricity system's dependability. System Operators (SO) in Texas, Denmark, Ireland, and Europe have recently been having problems with a greater degree of IBR penetration.

When there are comparatively few conventional synchronous generators and IBR penetration surpasses 50-60%, The issues get increasingly intricate. In order to address the problems of frequency stability in weak grids, the USA, UK, and Australia have recently undertaken programs to highlight trends in the power industry by including GFBESS. These power Electronics devices (Inverter Based Resources (IBRs)) are exploited to attain the goal of major issues like inertia, transient stability, frequency and voltage dip, power converter integration, and power oscillations [1-3]. The Grid-Following (GFL) control mechanism uses voltage profile and frequency.

The GFL techniques required a relation between voltage and angular rotational speed of SMs; as a result, there is decay in the attainment of desired responses like load sharing, load disturbance, drooping, effect of inertia, and voltage–frequency coordination [4]. To attain the desired response and eliminate the above-mentioned problems, Grid-Forming Converters (GFCs) are realized in the present power systems.

The use of GFCs to enhance system strength is examined by Zhou et al. [19], who show that GFCs can successfully handle problems with low system strength, such as sub-synchronous control interactions and voltage stability. The study emphasizes how crucial it is to properly build and tune

GFCs for certain applications. In this case, SMs and GFCs are expected to coordinate and maintain a stable system. The Droop Control technique imitates the functioning of the SGs and is considered to be a known control mechanism. These are classified in frequency-based droop [5, 6], angle-based droop [7, 8], and Power Synchronization Control (PSC) [9, 10]. Angle-based droop is used to eliminate the drawback of the frequency droop control mechanism of transient stability under the condition of voltage dips.

The transient instability occurs due to a change in active power value due to inverter current limitations and voltage reduction. Angle-based droop control employs the mechanism of using the inverter power angle to calculate the switching frequency of the inverter, which enhances the transient performance stability under current limitations. The Power-Synchronization Control (PSC) mechanism works based on a Phase-Locked Loop (PLL) to generate the switching frequency of the inverter and, as a result, can integrate the inverter with the grid more precisely [11].

Power electronics-based inverters like grid forming inverters, grid following inverters or solar inverters are very sensitive to the current fluctuation during the condition of fault, over current or load disturbances. In this case it is important to provide the current limitation techniques on the inverter side for the protection purpose of electronic devices like MOSFET / IGBT. Enhancing the dynamic synchronization capability of GFIs has been the main focus of recent developments in GFM control techniques. Ojo et al.'s assessment covers a number of control techniques, including virtual oscillator control, virtual synchronous machine control, and droop control [20]. The study highlights how current-limiting algorithms prevent current overloads and preserve operating margins between voltage and current control loops.

The research papers [10-14] have provided insight into the importance of current limitations. However, issues must be resolved, including transient over-voltage, undesirable current saturation, momentary over-current, and an unknown output current vector angle. This paper implements the AC current limitation technique at the AC side of the inverter. When the limit has been set according to the inverter's IGBT power rating capabilities and the reference current from the voltage control loop is applied to the saturation current.

This controlled current has been passed through the current control loop before generating the switching signals for the GFI in case of load disturbance. Strategy is implemented at low-level cascaded control design in dq-coordinates. The researchers of papers from [12-14] have worked on GFI dynamics connected to the ideal three-phase voltage source to supply the common load. In this paper, the performance analysis of GFI is implemented on a MATLAB model with the actual Synchronous generator dynamics when connected in parallel with GFI to supply the load demand on the grid. This research will help to deal with the practical condition of integrating power electronics-based resources with SG.

The article is formulated as follows: section-II describes the modelling of the SGs with excitation Systems. Section III covers the modelling of a grid-forming inverter using switching logic. Section IV describes the AC limitation technique to minimize load disturbance. Results and Conclusion are stated in Sections V and VI, respectively.

2. Modelling of SGs, Excitation Systems And PSS

This section comprises mathematical modelling of the system consisting of Grid Forming Inverter and Synchronous Generator. The dynamic model of systems consisting of mathematical differential equations for each subsystem is applied for simulation purposes in MATLAB. Here, both the systems GFI and SGs are called converter systems as mechanical energy is converted into AC electrical energy in the case of SGs and electric/electrochemical energy from the battery for GFI.

Combined systems are divided into two categories: (1) Systems with SGs and (2) Systems with GFI. Systems elements consisting of the synchronous generator consist of energy supplied to the shaft of the SGs in the form of mechanical energy. Mechanical energy is generated by steam, hydro, or gases and applied to the turbine. Elements included in the systems at SG sides are the electrical to mechanical transducer, actuator, synchronous machine, termination load, and excitation systems, with the necessary feedback shown in Figure 1. Nomenclatures given in the block diagram are mentioned in the Appendix.

The Synchronous generator has been modeled with an appropriate design of gain parameters (K1 to K6) and various time constants as per the selected rating of SG. Tunning parameters K1 and K2 are essential to maintain the small signal stability, ensuring the generator does not lose synchronism after small disturbances. To maintain transient stability against sudden load changes, K3 and K6 are tuned. Tunning of K4 and K5 are critical for the excitation system.

The equations for these parameters have been listed from Equations (1) to (10). Together with the turbine governor system, excitation system, and power system stabilizer, tuning of these parameters has been accomplished for the intended operation of SG. However, the issues associated with the response time and parameter variations increase overall control complexities. Thus, tunning techniques like particle swam optimization genetic algorithm can be used to tune the controller gain parameters of synchronous generation dynamics. In this paper, the optimization of parameters tunning criteria is not included.

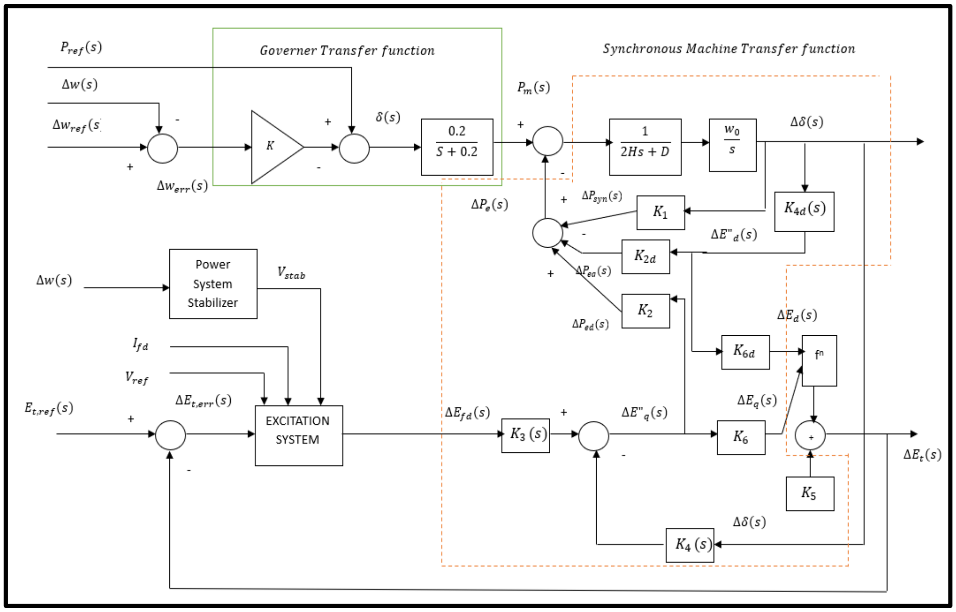

Fig. 1 Block diagram representation of synchronous machine with excitation systems

However, the nickolus and zigler method is used for the coarse tuning these parameters.

It has been achieved for the desired operation of SG along with the turbine governor system, excitation system and power system stabilizer.

$$K_1 = \frac{V_{\infty d0}^2}{X_d^* + X_{tl}} + \frac{V_{\infty d0}^2}{X_q^* + X_{tl}} - I_{q0}V_{\infty q0} + I_{d0}V_{\infty d0} \tag{1}$$

$$K_2 = \frac{V_{\infty d0}}{X_d^* + X_{tl}} \tag{2}$$

$$K_{2d} = \frac{V_{\infty q0}}{X_q^* + X_{tl}} \tag{3}$$

$$K_3(s) = \frac{1}{D(s)}(1 + \tau_{d0}^*)(X_d^* + X_{tl}) \tag{4}$$

$$K_4(s) = \frac{V_{\infty d0}}{D(s)}[(X_d - X_d^*) + \{(X_d' - X_d^*)\tau_{d0}' + (X_d - X_d')\tau_{d0}^*\}s] \tag{5}$$

$$K_{4d}(s) = \frac{C_{4d}}{1+\tau_q^* s} \tag{6}$$

$$K_5 = \left[\frac{E_{td0}}{E_{t0}} \cdot \frac{X_q^* V_{\infty q0}}{X_q^* + X_{tl}} - \frac{E_{tq0}}{E_{t0}} \cdot \frac{X_d^* V_{\infty d0}}{X_d^* + X_{tl}}\right] \tag{7}$$

$$K_6 = \left[\frac{E_{tq0}}{E_{t0}} \cdot \frac{X_{tl}}{X_d^* + X_{tl}}\right] \tag{8}$$

$$K_{6d} = \left[\frac{E_{td0}}{E_{t0}} \cdot \frac{X_{tl}}{X_q^* + X_{tl}}\right] \tag{9}$$

$$\tau_q^* = \left[\frac{X_q^* + X_{tl}}{X_q + X_{tl}}\right]\tau_{q0}^* \tag{10}$$

The a need for an excitation system and power system stabilizer to maintain the generator voltage stability and damp out the oscillation, especially when there is a load change. The transfer function of excitation systems and power system stabilizers are mentioned in Figures 2 and 3, along with the necessary equations.

Where The filter time constant is represented by T_R while T_A, T_B, T_C are the voltage regulator time constants and K_A is the voltage regulator Gain [22].

$$\Delta E_{efd}(s) = \frac{1+ST_C}{1+ST_B} * \frac{K_A}{1+ST_A} * \Delta E_{terr}(s) \tag{11}$$

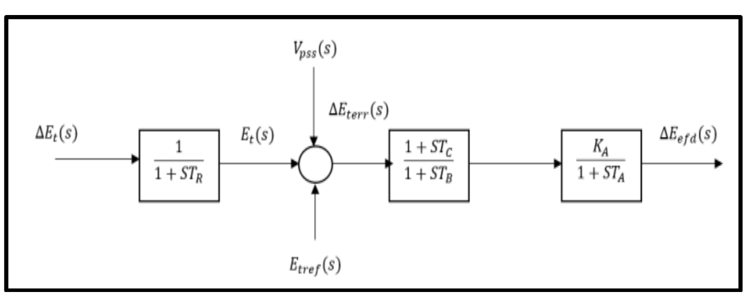

Fig. 2 Excitation system transfer

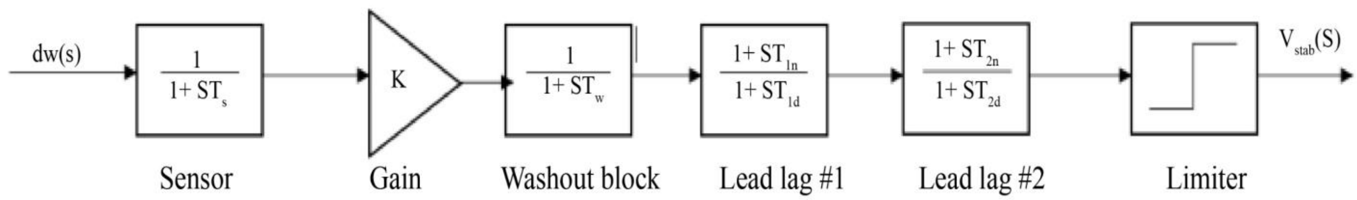

Fig. 3 Block diagram of power system stabilizer

$$V_{stab}(s) = \frac{1}{1+ST_s} * K * \frac{1}{1+ST_W} * \frac{1+ST_{1n}}{1+ST_{1d}} * \frac{1+ST_{2n}}{1+ST_{2d}} * dw(s) \quad (12)$$

$$V_{stab} > 0.3 = V_{stab} = V_{max} \ \& \ V_{stab} < 0.3 = V_{stab} = V_{min} \quad (13)$$

The block diagram shown in Figure 3 above consists of a Sensor, Gain, washout block, two lead-lag filters, and a limiter. A power system stabilizer is necessary to maintain the stability of the rotor angle in Synchronous Generators (SGs). The rotor angle is sensed by the transducer block. Then, after the washout filter (known as the high pass filter) is used, the time constant of the washout filter must be selected carefully, as it is the high pass filter used for system synchronization. Lead lag filters are used for phase compensation. The representation of the PSS output logic linked to the generator's active power output is made possible by the PSS output logic subsystem. The threshold values that define a hysteresis are PSS_{on} and PSS_{off} [19].

3. Model Description of GFI

The main function of GFI, being electronic control, is to maintain power system stability in a grid-based AC system. The GFI works as a controlled voltage source, having the capability to stabilize voltage and frequency. The basic circuit of the 6-bus system, where the Synchronous machine is connected with a grid-forming inverter, is shown in Figure 5.

Power set point adjustments, droop control, voltage loop control, current loop control, and voltage switching control make up the GFI block. This block mechanism is required to synchronize voltage, and frequency stability arises due to inertia. The system diagram with the necessary equations is shown in Figure 4.

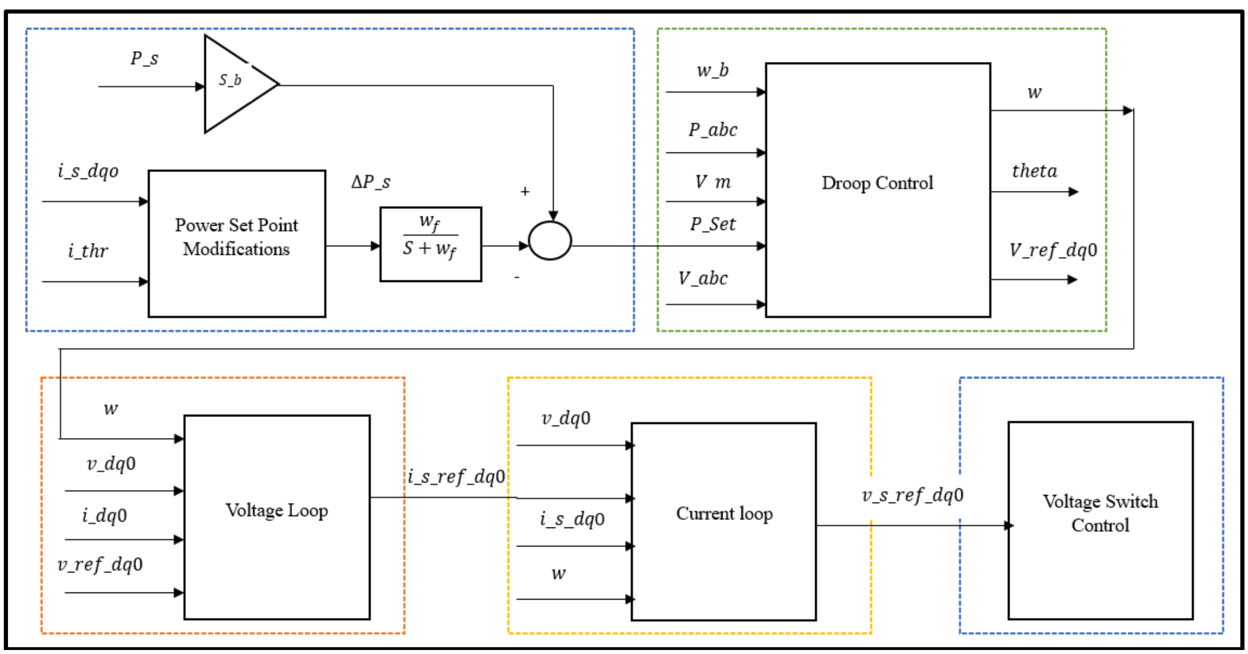

Fig. 4 GFI block diagram

The first block in the system is the power set point modification, which is to multiply with gain value to bring unit power into actual system power; the value of gain S_b is 100e6. Input to power set point blocks are two current values i_s_dqo, and i_thr, passing through mathematical operations results in output vector [PSet_d PSet_q 0]. The modified set point is given as input to the droop controller. In this, an application frequency-based droop control mechanism is implemented. There are linear relations between power and frequency, i.e., the inverter frequency decreases linearly with increasing power. These relations are defined using drooping coefficients [17].

$$Kp \rightarrow w = \frac{\Delta w}{\Delta P} \tag{14}$$

Droop controller is always used in association with a low-pass filter to filter out high-frequency harmonics. Since droop control is merely a type of proportional control, integral and derivative elements are added to enhance transient response. In the active power path, both derivative and integral terms are incorporated, while only the derivative term is incorporated in the reactive power path. The generated reference frequency is given as input to both the voltage and current loop. The functionality of the voltage loop is to generate reference current, which is given as input to the current loop, and the current loop generates voltage. The voltage generated from the current loop is given as reference voltage for switching semiconductor devices [18]. The switching logic of the semiconductor device (Voltage Switching Control (VSC)) implemented here is the reference voltage generated from the current loop output given as reference voltage to the VSC, which is an average model-based VSC. The constant current source is switched at a sampling interval of 0.001 sec, whose output is converted into voltage and given as input to VSC. The current value is generated for a constant current source based on the following equations.

A1 = (Vdc_n -Vdc) *k_dc
A2 = K_p*P_set
A3 = Kp*$\frac{w\_f}{s+w\_f}$*(P_s_abc - P_abc)
A4 = K_r*V_dc
S = A1+A2+A3+A4

Here, A1 is voltage difference multiplied by a gain, A2 is reference power multiplied by a gain, A3 is the difference of set and actual power multiplied by a gain, A4 is actual DC voltage multiplied by a gain, and S is the sum of all terms.

Output S will be converted by the transducer into current output. Let name as

A6 =.$\frac{1}{\tau s+1}$*S.

$$A7 = \begin{cases} i\_ul & \text{if } A6 > i\_ul \\ i\_li & \text{if } A6 > i\_li \end{cases} \quad \text{else } A7=A6$$

A7 is a pulsating current sample at 0.001 sec, given as input to a constant current source and will generate voltage till the simulation end time.

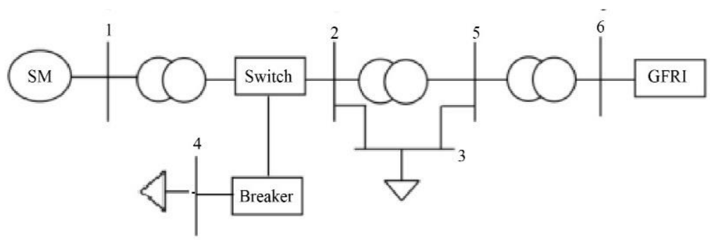

Fig. 5 6-bus test system with SM and GFI

4. Network Case Study and Synchronization of SG with GFI

As shown in Figure 5, the simulation of the 6-bus system is considered a test problem. The system comprises SM, transformers, transmission lines, circuit breakers, switches, termination load, and GFI. SM works on high inertia; as a result, there are major issues like transient stability, frequency and voltage dip, and power converter integration. To overcome the above problems, GFI works using semiconductor devices that have the flexibility to switch and synchronize AC power systems. To attain the above goal in GFI, a cascade control strategy is implemented, as shown in Figure 4. The AC system is simulated using the MATLAB simulation tool using the above control strategy. The system and design parameters of the whole system are mentioned in Tables 1 and 2.

Table 1. System parameters

System Components	Ratings
Synchronous generator	100 MVA, 13.8 KV, 50 Hz
Transformer 1	210 MVA, 50Hz, 13.8 KV/230 KV
Transformer 2	210 MVA, 50Hz, 230 KV/13.8KV
Transformer 3	100 MVA, 50Hz, 1KV/13.8KV
Transmission line 1	R= 4.4965 Ω, L= 0.1212 H
Transmission line 2	R= 16.928 Ω, L= 0.2711 H
Transmission line 3	R= 5.2900 Ω, L= 0.1431 H
Base load	At 230 KV, 50 HZ, 75 MW
Load disturbance	step load of 75 MW at 0.25 Sec
Shunt capacitance for transmission line in P.U.	C1= 1.00487, C2= 1.7058, C3= 1.3893 on the base of Cb= 6.1072 µF.
Grid forming inverter	V1rms =1 KV (on LV side of T/R-3), Ib_LV=8.165e4

	Vdc_n=2.4495 KV, (o/p of current control source) Vdc=2.42kv
Switching frequency	1 KHz
LC filter parameters	Rf= 5 μΩ, Lf= 1 μH, Cf= 0.06F

Table 2. Design parameters

Gain and Droop Controller Parameters	
Synchronous generator droop coefficient (Kp)	100 with 1% droop assumed
Pset	0.75 P.U.
Generator voltage regulator	Gain Ka=210, time constant Ta=0.001
DC source and governor-turbine time constants	τ_{dc} =0.05; τ_g =5
Grid Forming Inverter	
Droop control parameters	m_p=3.1416e-8
PI controller constants	K_p=0.001, K_i=0.5
AC voltage control gain parameters	ki_v_ac=2*0.25; kp_v_ac=0.001, Kff_v = 1, Kr=0.8333
Current loop control gain parameters	Kp_i =0.738891;Ki_i =(1/n)*1.19; Kff_i = 1;
AC current limiter set points	idppu=0.9; isatpu=1.2;

The results are shown in the following Figure 8. It consists of frequency and voltage plots. The simulation is run for 50 sec, and load disturbance is created at 25 sec. It shows that transients created by GFI are much lesser than SG, and its time is also faster. A novel current limiting technique is being introduced to minimize the effect of frequency and voltage fluctuations. The details of the current limit technique are discussed in the following section.

5. AC Current Limitation Technique

Transient instability may result in overcurrent in the power systems. To eliminate this problem and ensure the safety of the systems, the current limitation technique needs to be employed. The technique employed for limiting current during a large transient disturbance in a system is to saturate reference current [12, 21]. This AC current limiting block is added between the voltage and current control block, as shown in Figure 6. This indicates that the current has been controlled before going into the current control block, so the over-current on GFI can be avoided in case of load disturbance. Another technique imitates the effect of impedance and limits current when its value exceeds the nominal value. This technique is called limiting current based on variable virtual impedance [13-16]. Limiting AC current results in improved stability margin of systems. The strategy proposed in this approach of limiting AC current is scaling down the reference current i_s_ref_dq0 if it exceeds the already decided maximum current value i_max.

$$\text{i\_s\_ref\_dq0\_lim}= \begin{cases} \text{i\_s\_ref\_dq0} & \text{if i\_s\_ref\_dq0} < \text{i\_max} \\ k1 * \text{i\_s\_ref\_dq0} & \text{if i\_s\_ref\_dq0} > \text{i\_max} \end{cases} \tag{15}$$

$$k = \sqrt{(\text{i\_s\_ref\_d}^2 + \text{i\_s\_ref\_q}^2 + \text{i\_s\_ref\_0}^2)} \tag{16}$$

$$k1 = \frac{1}{K} \tag{17}$$

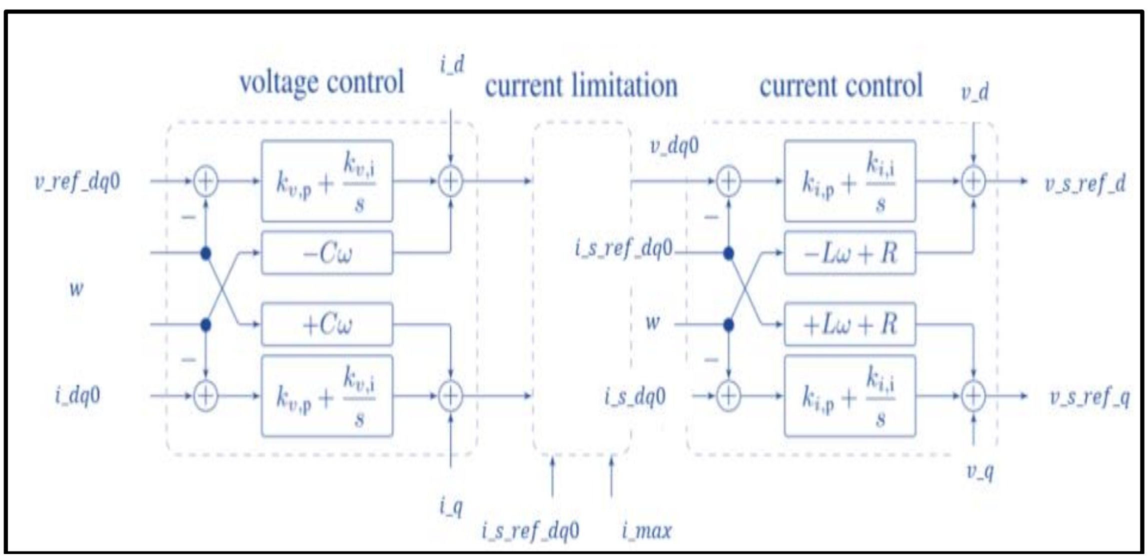

Fig. 6 Block diagram of current limitation

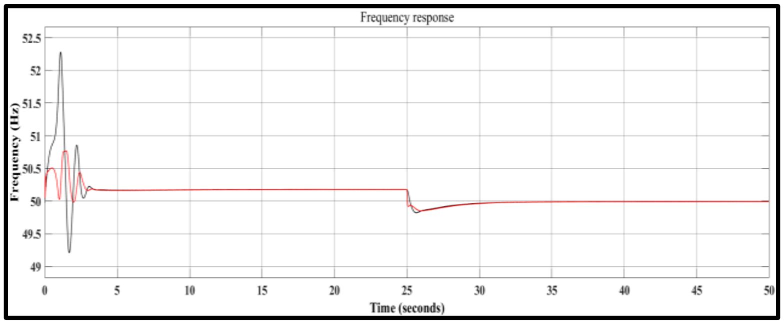

(a)

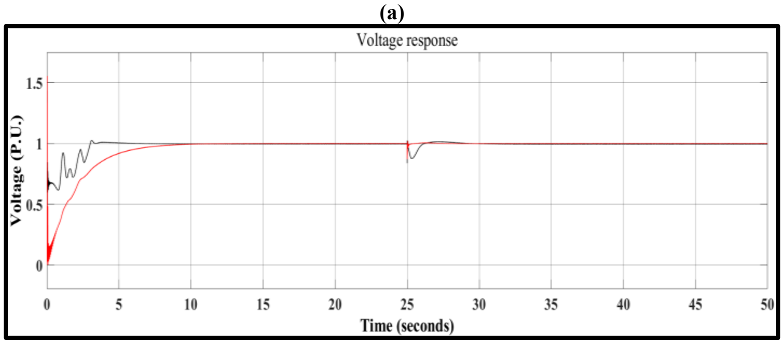

(b)

Fig.7(a) Frequency, and (b)voltage response without AC limiters.

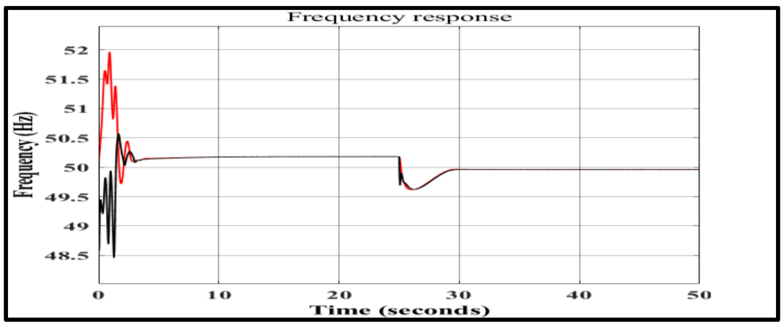

(a)

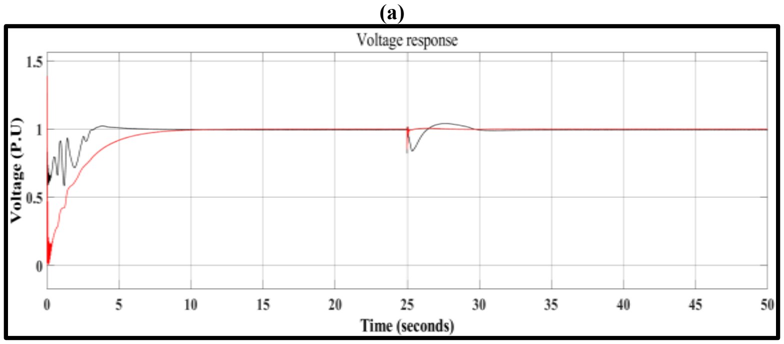

(b)

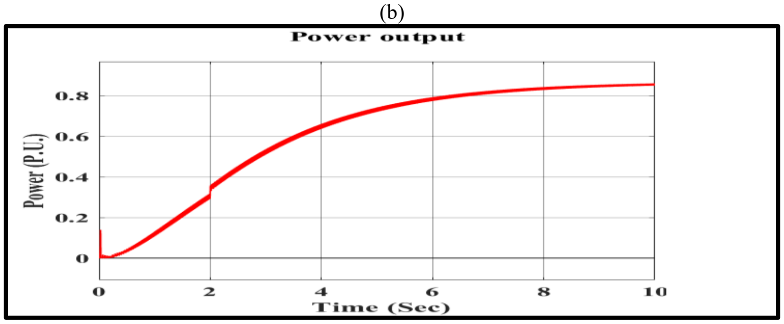

Fig. 8(a) Frequency, and (b)voltage response, (c)power output with AC limiters.

It has been seen from Figure 8 that by adding an AC limitation block, the transient response of GFI has been improved in terms of frequency and voltage parameters. In Figures (7) and (8), the black color graph shows the frequency and voltage response by SGs, and the red color graph shows the response by GFI. Overall, suppose the sensitivity analysis is carried out for the control parameters on the synchronous generator and GFI side. In that case, its impact on frequency and voltage stability, as well as power sharing capability, can be illustrated as: the W_f is the filter time constant that affects active power reference tracking and frequency stability during faults or step load increases. A higher value of droop gain mp will improve the damping but increase the frequency response, and its lower value will increase the risk of instability. Voltage control loop parameters K_{pv} and K_{iv} will affect the voltage recovery time after faults and more sensitivity to sudden reactive load changes. Control parameters K_{pi} and K_{ii} are critical for the current limitation response. The optimization of these control parameters is out of scope in this paper.

6. Results Analysis

In the 6-Bus system, the synchronous generator and grid-forming inverter are synchronized with the droop control method to supply a common load. The generator is 100MVA, and the GFI has a 50 MVA total capacity with 100 units of 500 KVA, each supplying a total load of 75 MW. Now, the load sharing is based on the capacity of SG and GFI. The load disturbance is created by adding 75 MW load at 25 sec. It has been observed from Figure 7 that transients created by GFI to supply an initial load of 75 MW are less compared to SG, where its ROCOF is 50.5 to 50.3 Hz at steady state and even though at 25 sec GFI frequency response is 50.3 to 49.85 Hz which gets settled down at new steady state value of 50 Hz in less than 2 sec.

Also, the voltage stability is achieved in less than 1.5 sec during load disturbance. After undertaking the current limiting technique, the frequency and voltage response are improved under current conditions when an additional load is inserted at 25 sec with a steady frequency of 50 Hz and voltage at 1.0 p.u. Also, by applying an AC current limiter with 1.2 P.U. of saturation current, a GFI can supply the total load even in the case of an outage of SG without overloading. Even though the results prove that the GFI, being a lower inertia system, responds faster than traditional SGs, the transients still come in the initial 2-3 seconds of time when both sources are synchronized. This can be improved by using the perfect tuning of control parameters and applying optimization techniques like PSO GA. This work will be taken up in the next research level.

7. Conclusion

The problem of six bus AC systems synchronization with SM and GFI is considered. The primary goal is to reduce the frequency and voltage instability brought on by the higher inertia of SM. The AC system is first simulated without current limitation and then after with current limitation techniques. It has been observed that frequency and voltage deviation are comparatively lower with the current limiting technique.

However, applying directly current limiting techniques without considering the whole system's dynamics strongly affects the system's stability. The strong and effective AC current limiting techniques can be designed by carefully tuning the controllers used in cascaded blocks, including the current limiting block. Hence, the AC current limiting technique and fine-tuning is still an open research problem as it may affect the load induced over current and grid faults.

References

[1] Rick Wallace Kenyon et al., "Stability and Control of Power Systems with High Penetrations of Inverter-based Resources: An Accessible Review of Current Knowledge and Open Questions," *Solar Energy*, vol. 210, pp. 149-168, 2020. [CrossRef] [Google Scholar] [Publisher Link]

[2] Integrating Inverter-Based Resources into Low Short Circuit Strength Systems, North American Electric Reliability Corporation, 2017. [Online]. Available: https://www.nerc.com/comm/RSTC_Reliability_Guidelines/Item_4a._Integrating _Inverter-Based_Resources_into_Low_Short_Circuit_Strength_Systems_-_2017-11-08-FINAL.pdf

[3] Wenzong Wang et al., "Instability of PLL Synchronized Converter-based Generators in Low Short-Circuit Systems and the Limitations of Positive Sequence Modeling," *North American Power Symposium*, Fargo, ND, USA, pp. 1-6, 2018. [CrossRef] [Google Scholar] [Publisher Link]

[4] ENTSO-E, "*High Penetration of Power Electronic Interfaced Power Sources (HPoPEIPS)*," ENTSO-E Guidance Document for National Implementation for Network Codes on Grid Connection, Technical Report, 2017. [Publisher Link]

[5] Karel De Brabandere et al., "A Voltage and Frequency Droop Control Method for Parallel Inverters," *IEEE Transactions on Power Electronics*, vol. 22, no. 4, pp. 1107-1115, 2007. [CrossRef] [Google Scholar] [Publisher Link]

[6] T.L. Vandoorn et al., "Review of Primary Control Strategies for Islanded Microgrids with Power-Electronic Interfaces," *Renewable and Sustainable Energy Reviews*, vol. 19, pp. 613-628, 2013. [CrossRef] [Google Scholar] [Publisher Link]

[7] Ritwik Majumder et al., "Improvement of Stability and Load Sharing in an Autonomous Microgrid Using Supplementary Droop Control Loop," *IEEE Transactions on Power Systems*, vol. 25, no. 2, pp. 796-808, 2010. [CrossRef] [Google Scholar] [Publisher Link]

[8] Jiefeng Hu et al., "Virtual Flux Droop Method-A New Control Strategy of Inverters in Microgrids," *IEEE Transactions on Power Electronics*, vol. 29, no. 9, pp. 4704-4711, 2014. [CrossRef] [Google Scholar] [Publisher Link]

[9] Lidong Zhang, Lennart Harnefors, and Hans-Peter Nee, "Power-Synchronization Control of Grid-Connected Voltage-Source Converters," *IEEE Transactions on Power Systems*, vol. 25, no. 2, pp. 809-820, 2010. [CrossRef] [Google Scholar] [Publisher Link]

[10] Lennart Harnefors et al., "Robust Analytic Design of Power-Synchronization Control," *IEEE Transactions on Industrial Electronics*, vol. 66, no. 8, pp. 5810-5819, 2019. [CrossRef] [Google Scholar] [Publisher Link]

[11] Ke Ji, Hong Lu, and Minxiao Wang, "A Vector-Power Synchronization Control for Grid-Forming Voltage-Source Converters with Enhanced Performance Under Wide SCR Condition," *IEEE Transactions on Power Delivery*, vol. 39, no. 4, pp. 2507-2519, 2024. [CrossRef] [Google Scholar] [Publisher Link]

[12] Iman Sadeghkhani et al., "A Current Limiting Strategy to Improve Fault Ride-through of Inverter Interfaced Autonomous Microgrids," *IEEE Transactions on Smart Grid*, vol. 8, no. 5, pp. 2138-2148, 2017. [CrossRef] [Google Scholar] [Publisher Link]

[13] Andrew D. Paquette, and Deepak M. Divan, "Virtual Impedance Current Limiting for Inverters in Microgrids with Synchronous Generators," *IEEE Transactions on Industry Applications*, vol. 51, no. 2, pp. 1630-1638, 2015. [CrossRef] [Google Scholar] [Publisher Link]

[14] Taoufik Qoria et al., "Current Limiting Algorithms and Transient Stability Analysis of Grid-Forming VSCs," *Electric Power Systems Research*, vol. 189, 2020. [CrossRef] [Google Scholar] [Publisher Link]

[15] Guillaume Denis et al., "The Migrate Project: The Challenges of Operating a Transmission Grid with Only Inverter-Based Generation. A Grid-Forming Control Improvement with Transient Current-Limiting Control," *IET Renewable Power Generation*, vol. 12, no. 5, pp. 523-529, 2018. [CrossRef] [Google Scholar] [Publisher Link]

[16] Xiongfei Wang et al., "Virtual-Impedance based Control for Voltage-Source and Current-Source Converters," *IEEE Transactions on Power Electronics*, vol. 30, no. 12, pp. 7019-7037, 2015. [CrossRef] [Google Scholar] [Publisher Link]

[17] Mukul Chandorkar, Deepak Divan, and Ram Adapa, "Control of Parallel Connected Inverters in Standalone AC Supply Systems," *IEEE Transactions on Industry Applications*, vol. 29, no. 1, pp. 136-143, 1993. [CrossRef] [Google Scholar] [Publisher Link]

[18] Nabil Mohammed et al., "Grid-Forming Inverters: A Comparative Study of Different Control Strategies in Frequency and Time Domains," *IEEE Open Journal of the Industrial Electronics Society*, vol. 5, pp. 185-214, 2024. [CrossRef] [Google Scholar] [Publisher Link]

[19] "IEEE Recommended Practice for Excitation System Models for Power System Stability Studies," *IEEE Std 421.5-2016 (Revision of IEEE Std 421.5-2005)*, pp. 1-207, 2016. [CrossRef] [Publisher Link]

[20] Xingyou Chen et al., "Transient Stability Analysis and Enhancement of Grid-Forming Converters: A Comprehensive Review," *Electronics*, vol. 14, no. 4, pp. 1-24, 2025. [CrossRef] [Google Scholar] [Publisher Link]

[21] Emmanuel Ebinyu et al., "Grid-Forming Control: Advancements towards 100% Inverter-Based Grids-A Review," *Energies*, vol. 16, no. 22, pp. 1-45, 2023. [CrossRef] [Google Scholar] [Publisher Link]

[22] Mads Graungaard Taul et al., "Current Limiting Control with Enhanced Dynamics of Grid-Forming Converters During Fault Conditions," *IEEE Journal of Emerging and Selected Topics in Power Electronics*, vol. 8, no. 2, pp. 1062-1073, 2020. [CrossRef] [Google Scholar] [Publisher Link]

[23] Prabha S. Kundur, *Power System Stability and Control*, McGraw-Hill, 2006. [Google Scholar] [Publisher Link]

APPENDIX

1. d, q,0 =Direct axis, Quadrature axis, open circuit Suffix
2. X_d , X_q = Direct axis & Quadrature axis synchronous reactance
3. X'_d, X'_q = Direct axis & Quadrature axis synchronous transient reactance
4. τ = Inertia Time constant
5. δ = Power angle of internal voltage w.r.f to terminal voltage in radian
6. D =Damping coefficient
7. H=Inertia Coefficient
8. P_m = Mechanical Power
9. P_e = Electrical Power
10. m = Measurement signal (12 element Vector)
11. a,b,c = 3 -phase terminals
12. τ'_{d0} = Direct axis open circuit transient time constant
13. τ'_{q0} = Quadrature axis open circuit transient time constant